An investigation of models of the IP_3R channel in *Xenopus* oocyte

J. W. Shuai,[1,a)] D. P. Yang,[1] J. E. Pearson,[2] and S. Rüdiger[3]
[1]*Department of Physics and Institute of Theoretical Physics and Astrophysics, Xiamen University, Xiamen 361005, China*
[2]*Applied Theoretical and Computational Physics, Los Alamos National Laboratory, Los Alamos, New Mexico 87545, USA*
[3]*Institute of Physics, Humboldt University Berlin, Newtonstr. 15, 12489 Berlin, Germany*

(Received 18 February 2009; accepted 29 May 2009; published online 18 September 2009)

We consider different models of inositol 1,4,5-trisphosphate (IP_3) receptor (IP_3R) channels in order to fit nuclear membrane patch clamp data of the stationary open probability, mean open time, and mean close time of channels in the *Xenopus* oocyte. Our results indicate that rather than to treat the tetrameric IP_3R as four independent and identical subunits, one should assume sequential binding-unbinding processes of Ca^{2+} ions and IP_3 messengers. Our simulations also favor the assumption that a channel opens through a conformational transition from a close state to an active state.
 [DOI: 10.1063/1.3156402]

The dynamics of inositol 1,4,5-trisphosphate (IP_3) receptor (IP_3R) channels is an important issue in cellular physiology and is central to many problems of cellular signaling. Models for calcium channels are widely used to investigate a variety of topics such as calcium oscillations and excitation-contraction coupling in cardiac cells. In particular, the mechanism that permits cells to organize regular calcium spikes in response to increased IP_3 levels is an intriguing issue of great interest for both the biological and physical communities. A crucial step in the analysis of IP_3 channels is the study of channel dynamics under (nonphysiological) conditions without Ca^{2+} feedback. Our work builds on recent patch clamp experiments for single IP_3 channels located in the nuclear membrane. We discuss different traditional and new IP_3R models by fitting their parameters to the stationary data of patch clamp recordings. Our analysis not only suggests that sequential binding-unbinding processes by Ca^{2+} ions and IP_3 messengers should be assumed but also supports the recent incorporation into the gating model of a ligand-independent conformational transition. An understanding of the single channel gating is fundamental to any further modeling approach of intracellular and intercellular calcium dynamics. This fact gives a central importance to the results presented in this work.

I. INTRODUCTION

Calcium is one of the most important messengers in the cytosol of living cells.[1] It can trigger and modulate a wide variety of calcium dependent signaling events and reaction cascades. A major mechanism of calcium signaling involves the liberation of Ca^{2+} ions from the endoplasmic reticulum (ER) through IP_3Rs.[2] Structurally, the IP_3R is a homomer with four subunits forming a single ion-conducting channel. The opening of the channel requires the binding of second messenger inositol 1,4,5-trisphosphate, which is generated in the cytoplasm in response to the binding of extracellular ligands to plasma membrane receptors. Gating of IP_3R is biphasically modulated by Ca^{2+} ions, such that small elevations of cytosolic Ca^{2+} concentration promote channel opening, whereas higher Ca^{2+} concentrations result in inactivation of the channel. This Ca^{2+} feedback, in addition to the clustered distribution of functioning IP_3Rs on the ER membrane, results in complex spatiotemporal Ca^{2+} signals, including Ca^{2+} puffs, saltatory waves, spreading waves, and spiral waves.[3]

Models of calcium signals play an important role to elucidate quantitatively the complex dynamics of various Ca^{2+} patterns generated by the IP_3 pathway. Because of the crucial role of IP_3R channels for the generation of calcium signals, an accurate IP_3R channel model is fundamental in order to simulate the calcium system properly.[4] Several IP_3R models[4–9] have been developed to describe experimental data obtained from IP_3R reconstituted in a bilayer membrane *in vitro*,[10] with the De Young–Keizer[5] model in particular being widely applied.

The intracellular calcium signals involve liberation through IP_3R from the ER. Although there is no single-channel experiment by now with IP_3R located on the ER membrane, IP_3R data were measured in different environments. Most recently patch-clamp recordings from native IP_3R in *Xenopus* oocyte nuclei have been obtained.[11,12] The experimental results indicate that there are significant differences in behavior of the reconstituted IP_3R in bilayer membrane[10] versus that of IP_3R in their native environment of the nuclear envelope in the *Xenopus* oocyte.[11,12] Although we do not know what exactly can be expected for IP_3R behavior on the ER versus that on the nuclear membrane, we take the available data as the closest estimate of the ER behavior. This assumption is supported by the fact that the ER membrane is physically connected to the nuclear membrane.

Therefore, we think that a suitable IP_3R model should be based on the recent data obtained on the nuclear membrane.

a)Telephone: (86) 592-218 2575. Electronic mail: jianweishuai@xmu.edu.cn.

TABLE I. The mismatch value for P_O fitting of the eight models. Here the value has been rescaled by the averaged open probability of the channel for the experimental data.

Model	8-state	6-state	9-state	7-state	13-state	20-state	21-state	46-state
Mismatch value	0.188	0.188	0.168	0.169	0.128	0.177	0.150	0.132

By now, only a few models have incorporated nuclear membrane data. Among these, an allosteric four-plus-two-conformation model was considered by Mak *et al.*[13] That model postulates that each of the four IP_3R monomers has one IP_3-binding site and three different functional Ca^{2+}-binding sites on the cytoplasmic side of the channel. Another model was developed by Baran,[14] consisting of one activation module and one inhibition module, both allosterically operated by Ca^{2+}, IP_3, and adenosine triphosphate (ATP), together with one adaptation module driven by IP_3 and Ca^{2+}. However, these models can predict only the steady-state gating properties and not the kinetics of individual channel openings and closings. A kinetic model, including an explicit dependence of channel gating with luminal calcium, was suggested by Fraiman and Dawson[15] to simulate a monomeric IP_3R. A further model, recently proposed by Shuai *et al.*,[16] contains a conformational change but is otherwise based on the De Young–Keizer model. The model successfully reproduces experimental estimates including the open probability, mean open and close times, and the multiexponential distributions of open and close time durations.

In this paper, we consider different types of IP_3R models and compare their data fitting to patch clamp data of IP_3R on the nuclear membrane in *Xenopus* oocyte.[11–13] In detail, in this study, we compare the data matching of various models to the open probability, mean open time, and mean close time of the channel as a function of calcium concentration and IP_3 concentration. We explore the behavior of IP_3R models by using the deterministic matrix transition analysis.[17,18] Our discussion suggests the inadequacy of De Young–Keizer-type models, which propose four independent and identical subunits. We conclude that the tetramerically structured IP_3R shows a sequential binding-unbinding process with Ca^{2+} ions and IP_3 messengers.

II. EXPERIMENTAL DATA OF IP_3R IN *XENOPUS* OOCYTE

The experimental data for IP_3R type-1 channels in nuclear membrane in the *Xenopus* oocyte have been obtained at various calcium concentrations C and IP_3 concentrations I.[11–13] The open probability P_O shows the following attributes. (1) At saturating IP_3 concentration, i.e., $I=10\ \mu M$, the channel exhibits a steep responding dynamics around $C=0.2\ \mu M$, changing from $P_O=0.13$ at $C=0.08\ \mu M$ to $P_O=0.73$ at $C=0.56\ \mu M$. (2) At $I=10\ \mu M$, for a large range of calcium concentration from $C=0.7\ \mu M$ to $25\ \mu M$, the channel shows a flat but large open probability around $P_O \sim 0.8$, indicating that calcium concentrations in this region are optimal. (3) At $I=10\ \mu M$, the channel shows a steep decrease in open probability with higher calcium concentration around $C=50\ \mu M$. (4) The channel also shows a very sensitive response to unsaturating IP_3 concentration around $I=0.02\ \mu M$, changing from $P_O=0.02$ at $I=0.01\ \mu M$ to $P_O=0.67$ at $I=0.033\ \mu M$ at calcium concentration around $1\ \mu M$.

The channel mean open time τ_O and mean close time τ_C were measured for saturating IP_3 concentration. The mean open times typically scatter around 8 ms at various calcium concentrations, except for the two extreme values at large and small calcium concentrations where the observed open times are small. For those two parameter regimes, however, the standard deviations are large. Thus, it is difficult to define a clear curve for τ_O as a function of C. As suggested by Mak *et al.*,[12,13] τ_O first increases monotonically with C, and after reaching the maximum around $C=2\ \mu M$, it monotonically deceases with C. However, in Ref. 15, the authors interpreted it simply as a constant τ_O, which is independent of C.

III. THE FITTING OF MODELS TO EXPERIMENTAL DATA

We consider various models by fitting the stationary open probability, mean open time, and mean close time to data obtained in experiments. To find an optimal fitting, all the model parameters were changed systematically in a reasonable region and the fitting results were judged by an evaluation function. In order to calculate the open probability, the only parameters we need are the reaction dissociation constants, while to determine the open time and close time, binding/unbinding rates are needed. For the experimental data, the open probability is given at varying Ca^{2+} concentrations with four different IP_3 concentrations, while the mean open and close times are given at $I=10\ \mu M$ only.

For the open probability P_O we consider the mismatch function

$$W_{P_O}=\sum_{I,C}\left|P_O^{\mathrm{expt}}(I,C)-P_O^{\mathrm{mod}}(I,C)\right| \tag{1}$$

to obtain the optimal fitting parameters of all the reaction dissociation constants in the model. The mismatch values for P_O fitting with various IP_3R models are given in Table I. Further, we use the mismatch function

$$W_T=\frac{\Sigma_C\left|\tau_O^{\mathrm{expt}}(C)-\tau_O^{\mathrm{mod}}(C)\right|}{\Sigma_C\tau_O^{\mathrm{expt}}(C)}+\frac{\Sigma_C\left|\tau_C^{\mathrm{expt}}(C)-\tau_C^{\mathrm{mod}}(C)\right|}{\Sigma_C\tau_C^{\mathrm{expt}}(C)} \tag{2}$$

for τ_O and τ_C at $I=10\ \mu M$ to obtain the optimal fitting parameters of the binding rates. We notice that the open time duration experimentally is of the order of 10 ms, while the close time duration is distributed in the range of 1–2000 ms. To balance the contributions of open and close time in Eq.

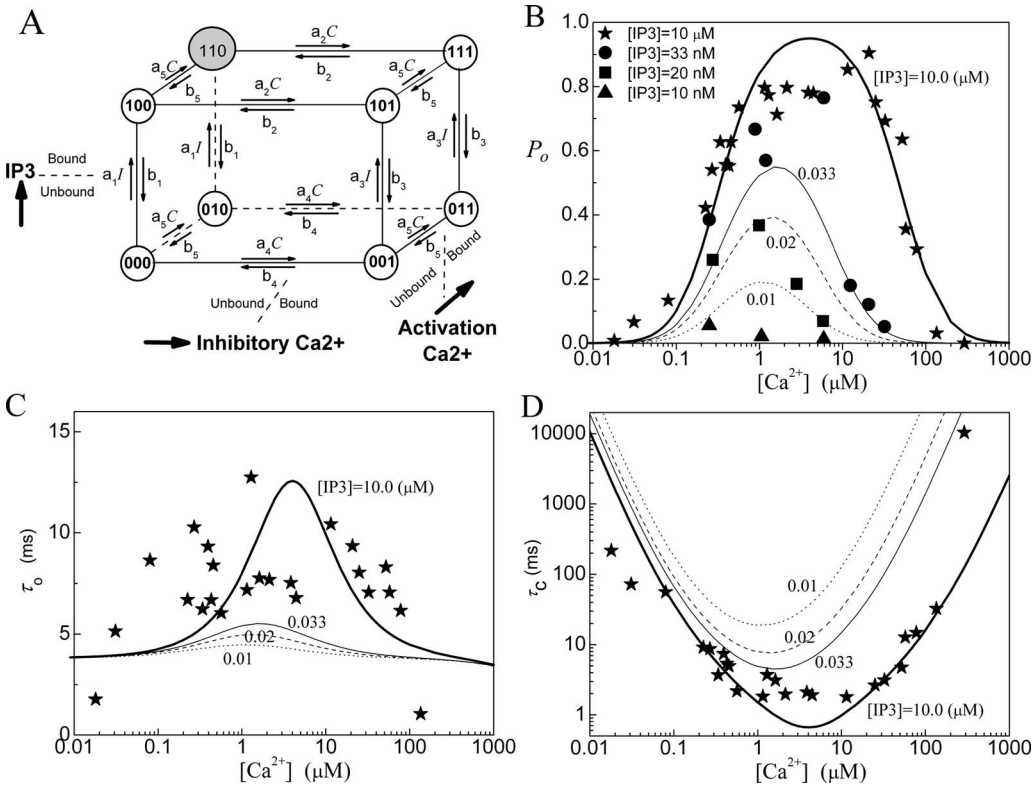

FIG. 1. Model 1: (a) The structure of the De Young–Keizer IP_3R subunit model. The graph shows the dependence of (b) the open probability P_O, (c) the mean open time τ_O, and (d) the mean close time τ_C as a function of Ca^{2+} concentration for different concentrations of IP_3. The lines show the results calculated with the deterministic transition matrix theory and the symbols show the results obtained from single-channel patch clamp from IP_3R on native nuclear membranes (Refs. 11–13). Here, thick lines and stars are for $[IP_3]=10$ μM, thin lines and circles are for 0.033 μM, dashed lines and squares are for 0.02 μM, and dotted lines and triangles are for 0.01 μM. Same notations are used in the following figures. The parameters used in the model are $K_1=0.0072$ μM, $K_2=78$ μM, $K_3=0.22$ μM, $K_4=K_1K_2/K_3$, $K_5=0.21$ μM, $a_1=500$ μM^{-1} s^{-1}, $a_2=0.01$ μM^{-1} s^{-1}, and $a_5=400$ μM^{-1} s^{-1}.

(2), we rescale the errors between the experimental and numerical data by the experimental results.

IV. THE DE YOUNG–KEIZER IP_3R MODELS

In many numerical simulations of Ca^{2+} signals, a widely applied IP_3R model is the De Young–Keizer model[5] as well as its simplified versions.[19,20] Therefore, in this section we will first discuss the fitting of the modified De Young–Keizer model to experimental data.

A. Model 1: IP_3R model with four 8-state subunits

The De Young–Keizer IP_3R model[5] comprises four identical and independent subunits. In each subunit, there are two independent Ca^{2+} binding sites (i.e., an activating binding and inhibitory binding site) and an IP_3 binding site. The state of each subunit is denoted as (ijk), where the index i represents the IP_3 binding site, j the activating Ca^{2+} binding site, and k the inhibitory Ca^{2+} binding site. An occupied site is represented by 1, and a nonoccupied site by 0. A schematic picture of the state transitions for De Young–Keizer IP_3R subunit is shown in Fig. 1. The channel is open when three or four subunits are in the (110) state.

For all binding/unbinding loops given in Fig. 1, the thermodynamic constraint of detailed balance requires that the reaction dissociation constants satisfy the relation $K_1K_2=K_3K_4$. In the model, each subunit has eight different states with transitions governed by second-order rate constants a_i for binding processes and first-order rate constants b_i for unbinding processes [Fig. 1(a)]. In order to calculate the channel open probability, the necessary parameters are the reaction dissociation constants, i.e., $K_i=b_i/a_i$, while the calculation of mean open time and mean close time requires the values of binding and unbinding rates. Parameter values needed for P_O, τ_O, and τ_C are given in the legend of Fig. 1.

Now we apply the deterministic matrix transition method[17,18] to analyze the channel open probability, mean open time, and mean close time. The probability of an IP_3R subunit being in state (ijk) is denoted by P_{ijk} with $\Sigma P_{ijk}=1$. By mass action kinetics, the equations describing the subunit dynamics are

$$\frac{dP}{dt}=PQ, \tag{3}$$

where Q is the generator matrix of transition rates and P is the vector of probability of subunits.

Mathematically, the equilibrium state is defined as $dP/dt=0$. The equilibrium vector w satisfies $wQ=0$ according to the transition matrix theory. Detailed balance is imposed so that we can solve for the vector w easily. This is done by calculating the probabilities in terms of their probabilities relative to state (000) along the shortest binding/unbinding path. These unnormalized probabilities are denoted as q_{ijk} with $q_{000}=1$. As an example, the equilibrium

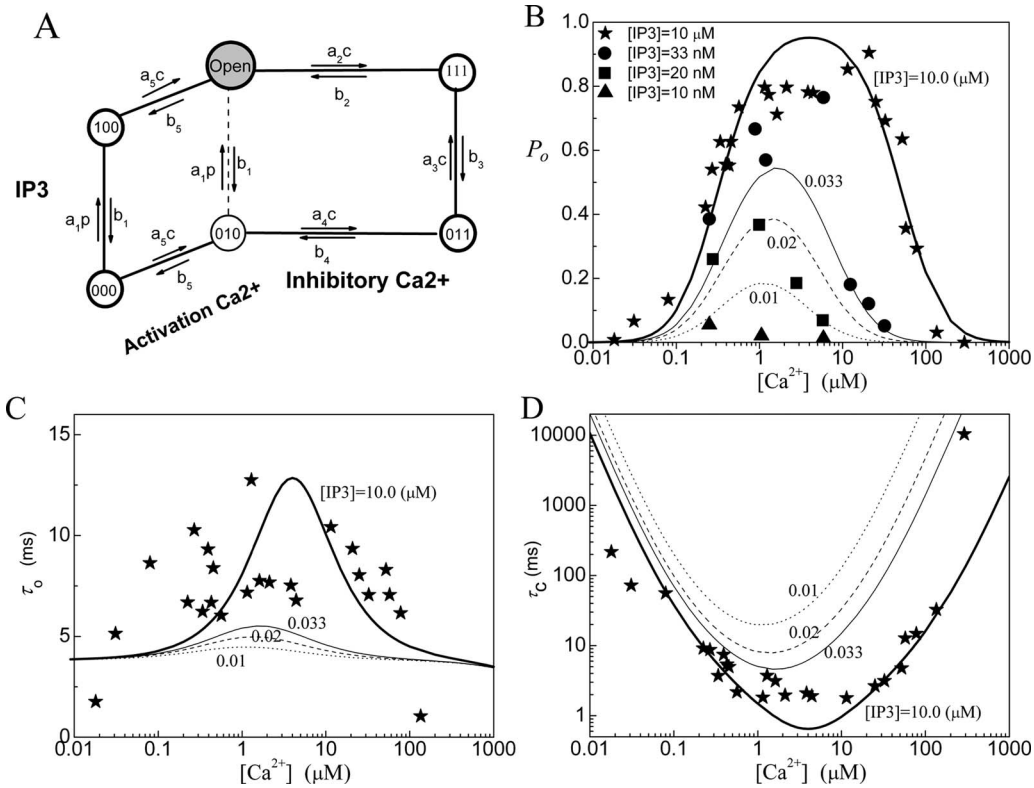

FIG. 2. Model 2: (a) The subunit structure of the channel model, (b) the open probability P_O, (c) the mean open time τ_O, and (d) the mean close time τ_C. In the model K_1=0.008 μM, K_2=78 μM, K_3=0.22 μM, $K_4=K_1K_2/K_3$, K_5=0.21 μM, a_1=400 μM^{-1} s^{-1}, a_2=0.01 μM^{-1} s^{-1}, and a_5=400 μM^{-1} s^{-1}.

probability (q_{110}) of state (110) relative to that of state (000) is just the product of forward to backward rates along any of the shortest paths connecting (000) to (110) (i.e., either through state 100 or state 010) given as

$$q_{110} = \frac{IC}{K_1 K_5}. \tag{4}$$

Then the normalized equilibrium probability for state (ijk) is

$$w_{ijk} = \frac{q_{ijk}}{Z}, \tag{5}$$

where Z is the normalization factor defined by $Z=\Sigma q_{ijk}$ and given as

$$Z = 1 + \frac{C}{K_4} + \frac{C}{K_5} + \frac{C}{K_4}\frac{C}{K_5} + \frac{I}{K_1} + \frac{I}{K_1}\frac{C}{K_2} + \frac{I}{K_1}\frac{C}{K_5} + \frac{I}{K_1}\frac{C}{K_2}\frac{C}{K_5}. \tag{6}$$

Thus, the normalized equilibrium probability for state (110) is as follows:

$$w_{110} = \frac{I}{K_1}\frac{C}{K_5}\frac{1}{Z}. \tag{7}$$

For the tetrameric IP_3R model, the channel opens when three out of four subunits are in state (110), so the channel open probability is written as

$$P_O = P_{4O} + P_{3O} = w_{110}^4 + 4w_{110}^3(1 - w_{110}) \tag{8}$$

with $P_{4O}=w_{110}^4$ and $P_{3O}=4w_{110}^3(1-w_{110})$.

Because channel states (110, 110, 110, not −110) are the only open states that connect to closed channel states by any one of three (110) states changing to the other three states, i.e., 100, 010, or 111 with rate b_5, b_1, or $a_2[Ca^{2+}]$, we can directly write the equilibrium probability flux between open and close states as follows:

$$J = 3P_{3O}(b_1 + b_5 + a_2 C). \tag{9}$$

The mean open and close times are then given by

$$\tau_O = \frac{P_O}{J}, \qquad \tau_C = \frac{1 - P_O}{J}. \tag{10}$$

The fittings of the channel model to the experimental data are shown in Figs. 1(b)–1(d) for P_O, τ_O, and τ_C. For the fitting of P_O at I=10 μM, the model does not provide a flat P_O for calcium concentrations changing from C=0.7 to 25 μM. The model also fails to give a steep response to IP_3 concentration changes around I=0.02 μM. A calcium concentration dependent τ_O is clearly obtained from the model.

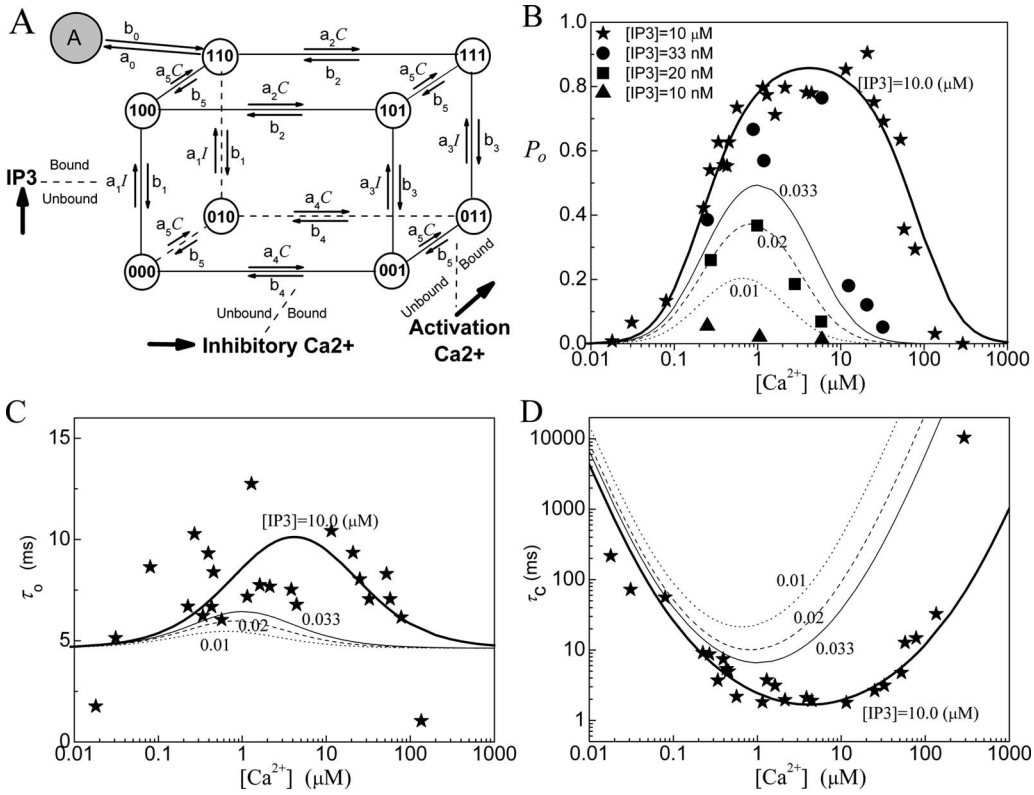

FIG. 3. Model 3: (a) The subunit structure of the channel model. A conformational transition to an active state (state-A) occurs before the subunit can contribute to channel opening. (b) The open probability P_O, (c) the mean open time τ_O, and (d) the mean close time τ_C. In the model $K_1=0.0054$ μM, $K_2=17.6$ μM, $K_3=0.64$ μM, $K_4=K_1K_2/K_3$, and $K_5=1.04$ μM. For the conformational change, $K_0=0.135$ μM and $a_0=535$ μM^{-1} s^{-1}.

B. Model 2: IP$_3$R model with four 6-state subunits

Now we consider a simplified De Young–Keizer IP$_3$R model in which each subunit has six states only, as shown in Fig. 2. The channel is open when three or four identical and independent subunits are in the (110) state.

For this model, the normalization factor is written as

$$Z = 1 + \frac{C}{K_5} + \frac{I}{K_1} + \frac{C}{K_4}\frac{C}{K_5} + \frac{I}{K_1}\frac{C}{K_5} + \frac{I}{K_1}\frac{C}{K_2}\frac{C}{K_5}. \tag{11}$$

The other formulas are the same as those for model 1.

The fittings of the channel model to the experimental data are given in Figs. 2(b)–2(d) for P_O, τ_O, and τ_C. One can see that the fitting results of this model are quite similar to the fittings of model 1. As given in Table I, the mismatch values for P_O fitting are 0.188 for both model 1 and model 2. It appears that the states and transitions omitted in the derivation of model 2 from model 1 are not essential for the gating behavior.

V. IP$_3$R MODELS WITH CONFORMATIONAL CHANGE DYNAMICS

A. Model 3: IP$_3$R model with four 9-state subunits

In Ref. 16, we have proposed a modified De Young–Keizer IP$_3$R model. The model comprises four identical and independent subunits. Two independent Ca^{2+} binding sites for each subunit (i.e., an activating binding and inhibitory binding site) and an IP$_3$ binding site, are assumed for each subunit. The model further includes a conformational change whereby a subunit in the (110) state (one IP$_3$ and one activating Ca^{2+} bound) is "inactive" and must change through a conformational transition to an "active" (A) state before it can contribute to channel opening. This conformational step is analogous to the well-characterized behavior of nicotinic acetylcholine receptors[21] and further implies that the active state is locked with respect to agonist binding and dissociation. The model also assumes that the channel is open when either three or four subunits are in active state. A schematic picture of the state transitions for a subunit is shown in Fig. 3(a) and the fitting results are shown in Figs. 3(b)–3(d). Notice that the parameters obtained here are slightly different from those in Ref. 16, where the optimized fitting process was not used. As shown in Table I, the open probability is better fitted with this model than with the models 1 and 2. This supports our assumption that a channel opens through a conformational transition from a close state to an active state.

B. Model 4: IP$_3$R model with four 7-state subunits

Now we consider a simplified IP$_3$R model based on model 3. In the model, each subunit has seven states, as shown in Fig. 4. For this model, the equilibrium probability for the active state (i.e., A-state) is given as

$$w_A = \frac{I}{K_1}\frac{C}{K_5}\frac{1}{K_0}\frac{1}{Z} \tag{12}$$

with

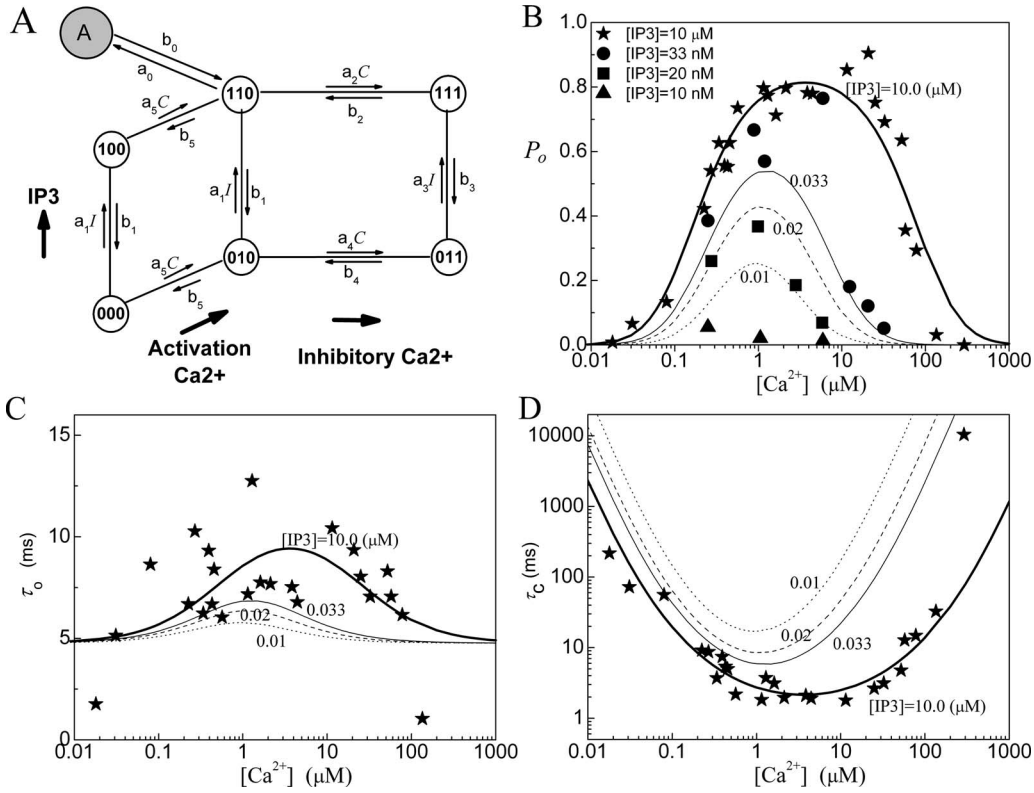

FIG. 4. Model 4: (a) The subunit structure of the channel model, (b) the open probability P_O, (c) the mean open time τ_O, and (d) the mean close time τ_C. In the model K_1=0.018 μM, K_2=24 μM, K_3=0.4 μM, $K_4=K_1K_2/K_3$, K_5=0.56 μM, and K_0=0.194 μM with a_0=360 μM^{-1} s^{-1}.

$$Z = 1 + \frac{C}{K_5} + \frac{I}{K_1} + \frac{I}{K_1}\frac{C}{K_2} + \frac{I}{K_1}\frac{C}{K_5} + \frac{I}{K_1}\frac{C}{K_2}\frac{C}{K_5} + \frac{I}{K_1}\frac{C}{K_5}\frac{1}{K_0}. \tag{13}$$

The equilibrium probability flux between open and close states is given as

$$J = 3b_0P_{3O}. \tag{14}$$

The other formulas are the same as those for model 1.

The fittings of the channel model to the experimental data are given in Figs. 4(b)–4(d) for P_O, τ_O, and τ_C. In fact, the fittings of this model are quite similar to the fittings of model 3. Compared to the results given by model 1 and model 2, model 3 and model 4 give a better fitting of P_O at optimal calcium concentrations around C=2 μM at I =10 μM. However, the model also fails to give a sensitive response to IP_3 concentrations around I=0.02 μM. Again, model 3 and model 4 give a similar approximation of the experimental data, suggesting that the two omitted states are inessential.

C. Model 5: IP_3R model with four 13-state subunits

The above four models all show a low sensitivity in response to I around 0.02 μM. In order to obtain a sensitive response of the channel to IP_3 concentration, we consider a 13-state subunit IP_3R model.

The model comprises four identical and independent subunits. We still consider two independent Ca^{2+} binding sites for each subunit, i.e., an activating binding site and an inhibitory site. However, in order to account for the observed strongly cooperative dependence of IP_3R channel opening on I, we assume that there are two IP_3 sequential binding sites in each subunit. A schematic picture of the transitions among 13 states for each subunit is shown in Fig. 5(a). The channel is open when either three or four subunits are in the active state.

For this model, the normalization factor Z is a sum of 13 terms that can be easily written out and we have

$$w_A = \frac{I}{K_1}\frac{I}{K_1}\frac{C}{K_5}\frac{1}{K_0}\frac{1}{Z}. \tag{15}$$

The other formulas are the same as those for model 4. The fittings of the channel model to the experimental data for P_O, τ_O, and τ_C are given in Figs. 5(b)–5(d). As a comparison of Fig. 5 with Figs. 1–4, one can see that a more sensitive response of the channel for P_O to IP_3 concentration can be obtained with model 5. As shown in Table I, compared to the previous four models, a better fitting for the open probability is obtained with this model.

Each monomer of the tetrameric channel complex has two IP_3 binding sites with different dissociation constants, as has also been suggested in Ref. 6. However, the molecular structure study of the IP_3R indicates that there is one IP_3 core binding domain and several calcium binding sites for each monomer.[2,22] Thus the experimental data do not favor the assumption of two IP_3 binding sites for each subunit. However, this model clearly shows that a sequential binding of IP_3 messengers can give a steep change in P_O versus I.

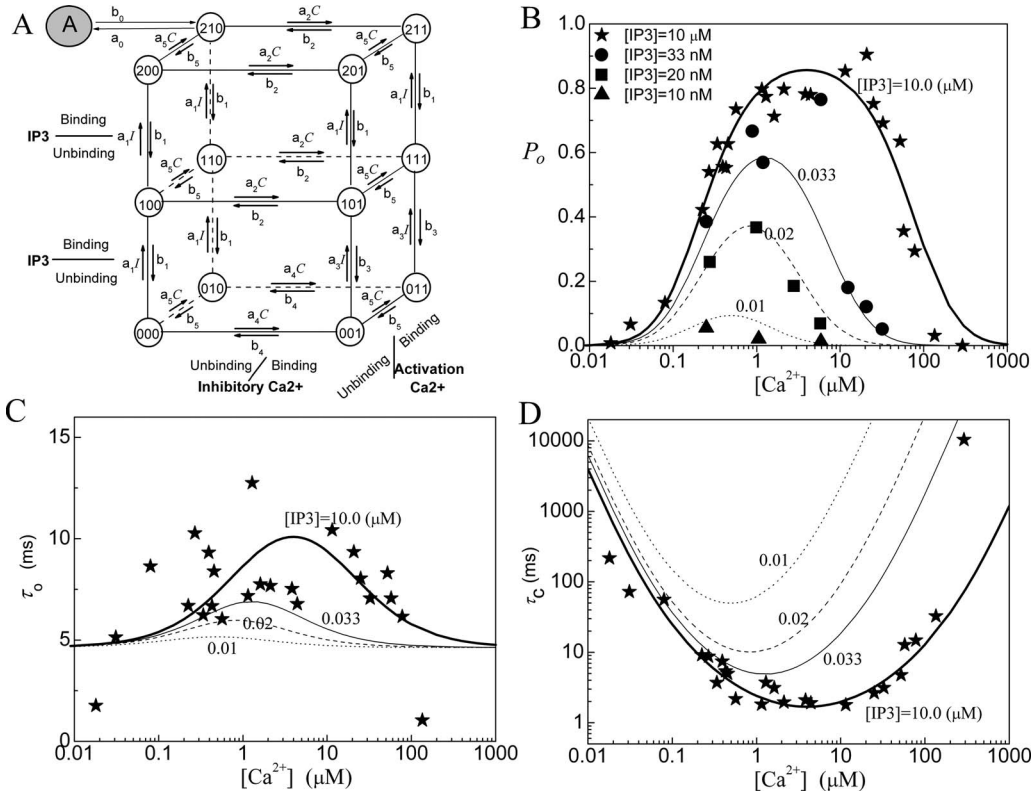

FIG. 5. Model 5: (a) The subunit structure of the channel model, (b) the open probability P_O, (c) the mean open time τ_O, and (d) the mean close time τ_C. In the model $K_1=0.005\ \mu$M, $K_2=15.6\ \mu$M, $K_3=2.25\ \mu$M, $K_4=K_1K_2/K_3$, $K_5=1.01\ \mu$M, and $K_0=0.135\ \mu$M with $a_0=535\ \mu\text{M}^{-1}\ \text{s}^{-1}$.

VI. SEQUENTIAL BINDING IP$_3$R MODELS

A. Model 6: 20-state IP$_3$R model

In contrast to the five models discussed above—with the assumption of four independent units—we will now consider the tetrameric IP$_3$R channel as a single unit with sequential binding processes. In the model, we assume that there are only two sequential activating Ca^{2+} binding sites and only one inhibitory Ca^{2+} binding site. There are four sequential IP_3 binding sites. We assume that only after the two activating binding sites are occupied by Ca^{2+} ions, the inhibitory Ca^{2+} binding site becomes available. Further, only after the inhibitory Ca^{2+} binding site becomes empty, the unbinding processes for activating Ca^{2+} ion can occur sequentially. The Ca^{2+} binding/unbinding processes are independent of the IP_3 binding/unbinding processes. A schematic picture for the transitions among the 20 channel states is shown in Fig. 6(a). The channel is open when it is in state (420) with four IP_3 messengers bound to the IP_3 sites and two Ca^{2+} ions bound to the activating sites.

For this model, the normalization factor Z is a sum of 20 terms and we have

$$w_{420}=\left(\frac{I}{K_1}\right)^4\left(\frac{C}{K_5}\right)^2\frac{1}{Z}. \tag{16}$$

Obviously, we also have

$$P_O=w_{420}, \tag{17}$$

$$J=P_O(b_1+b_5+a_2C), \tag{18}$$

and so

$$\tau_O=\frac{P_O}{J}=\frac{1}{b_1+b_5+a_2C}. \tag{19}$$

The fittings of the channel model 6 to the experimental data are given in Figs. 6(b)–6(d) for P_O, τ_O, and τ_C. For the fitting of P_O at $I=10\ \mu$M, the model could not supply a flat P_O at optimal calcium concentration. The model fails to exhibit a steep decreasing P_O with large C at $I=10\ \mu$M. With this model, as given by Eq. (19), τ_O almost stays constant for $C<2\ \mu$M and then decreases at large C.

B. Model 7: 21-state IP$_3$R model

Next, based on model 6, we furthermore consider the conformational change dynamics at state (420) for the channel to become open. A schematic picture for the transitions among the 21 states is shown in Fig. 7(a). With $J=b_0P_O$, we have a simple result for the mean open time as $\tau_O=1/b_0$, which is independent of any concentrations.

The fittings of the channel model 7 to the experimental data are shown in Figs. 7(b)–7(d) for P_O, τ_O, and τ_C. After considering the conformation change, the model can provide a flat P_O at optimal calcium concentration and also increases the sensitivity of P_O to I at optimal C. However, the model still fails to give a steep decreasing P_O with large C at $I=10\ \mu$M. This failure occurs because only one inhibitory Ca^{2+} binding site is assumed in the model.

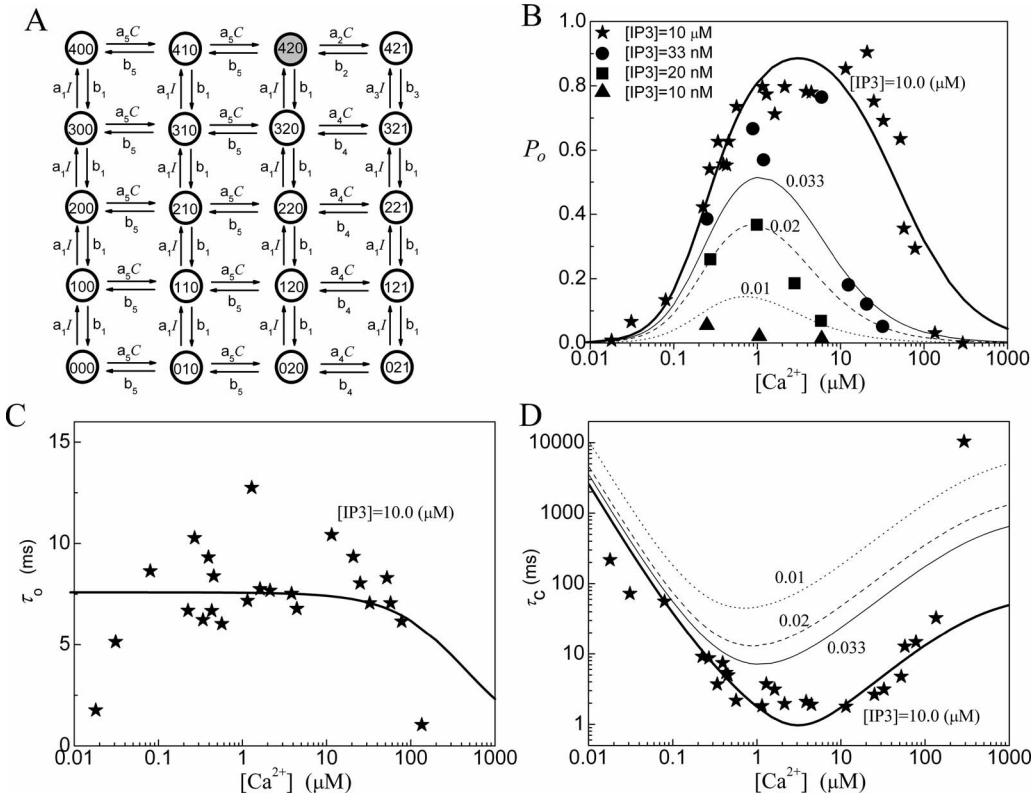

FIG. 6. Model 6: (a) The state structure of the sequential binding IP_3R model, (b) the open probability P_O, (c) the mean open time τ_O, and (d) the mean close time τ_C. In (c), the mean open time is independent of IP_3 concentration. In the model $K_1=0.009$ μM, $K_2=48$ μM, $K_3=0.3$ μM, $K_4=K_1K_2/K_3$, $K_5=0.18$ μM, $a_1=240$ μM^{-1} s^{-1}, $a_2=0.3$ μM^{-1} s^{-1}, and $a_5=720$ μM^{-1} s^{-1}.

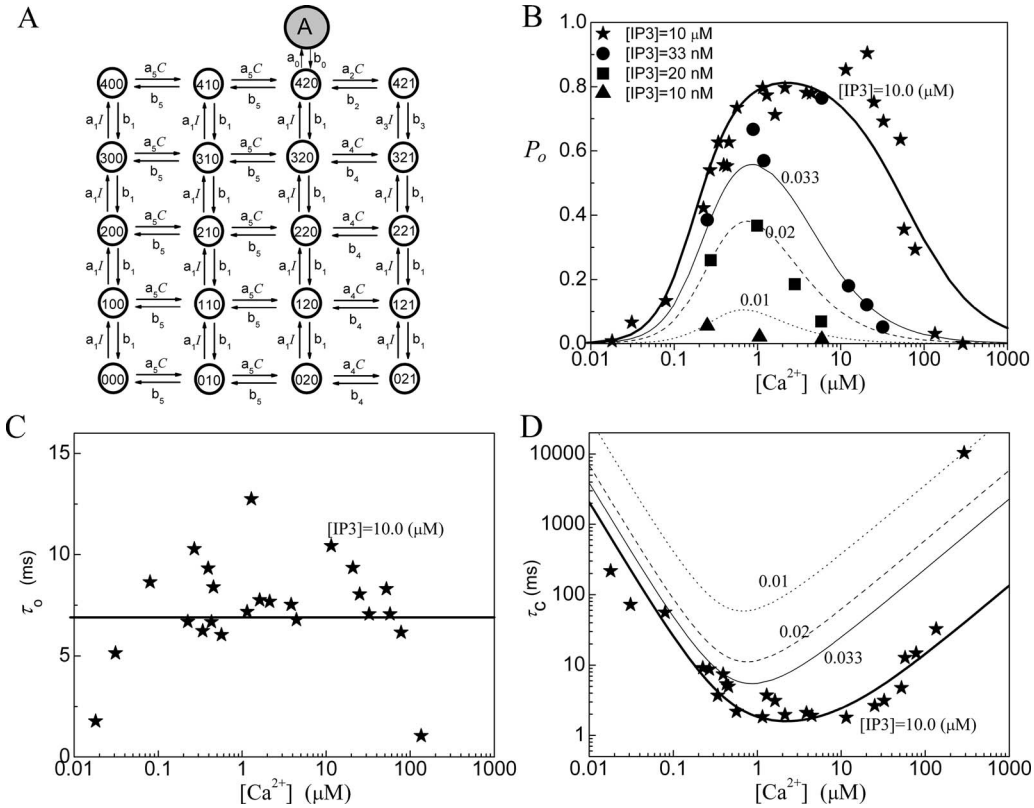

FIG. 7. Model 7: (a) The state structure of the sequential binding IP_3R model, (b) the open probability P_O, (c) the mean open time τ_O, and (d) the mean close time τ_C. In the model $K_1=0.016$ μM, $K_2=8$ μM, $K_3=0.3$ μM, $K_4=K_1K_2/K_3$, $K_5=0.44$ μM, and $K_0=0.151$ μM with $a_0=960$ μM^{-1} s^{-1}.

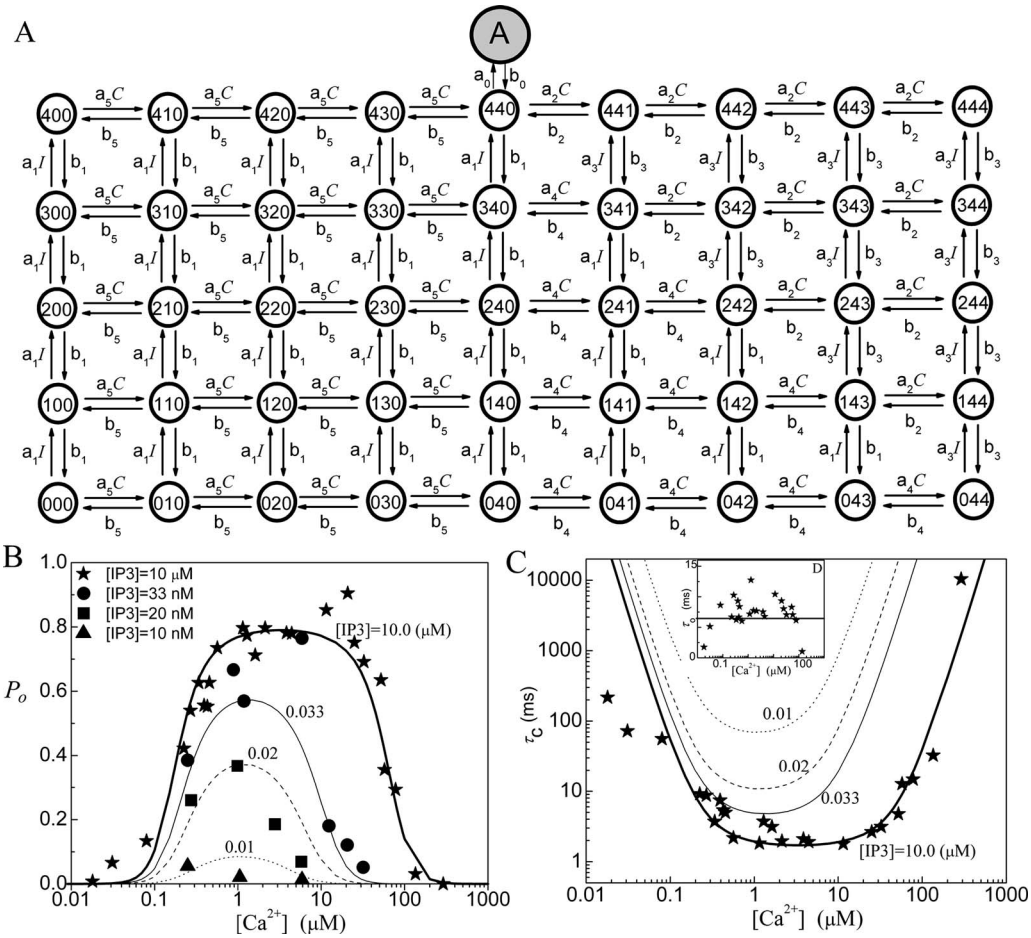

FIG. 8. Model 8: (a) The state structure of the sequential binding IP$_3$R model, (b) the open probability P_O, and (c) the mean close time τ_C. The inset figure in (c) is the plot of the mean open time τ_O. In the model K_1=0.02 μM, K_2=53 μM, K_3=0.2 μM, $K_4=K_1K_2/K_3$, K_5=0.21 μM, and K_0=0.233 μM with a_0=155 μM^{-1} s^{-1}.

C. Model 8: 46-state IP$_3$R model

In this model, we consider four sequential activating Ca^{2+} binding sites, four sequential inhibitory Ca^{2+} binding sites, and four sequential IP_3 binding sites. Thus each monomer has one activating Ca^{2+} binding site, one inhibitory Ca^{2+} binding site, and one IP_3 binding site. We assume that only after the four activating binding sites are occupied sequentially by Ca^{2+} ions, the four inhibitory Ca^{2+} binding sites become available sequentially. Only after the inhibitory Ca^{2+} binding site becomes empty sequentially, the unbinding processes for activating Ca^{2+} ion can occur sequentially. The Ca^{2+} binding/unbinding processes and the IP_3 binding/unbinding processes are independent. We furthermore consider the conformational change dynamics at state (440) (i.e., with four activating Ca^{2+} and four IP_3 bound on the channel) for the channel to become open. Thus there are in total 46 states in this model. A schematic picture for the transitions among the 46 channel states is shown in Fig. 8(a). Similar to model 7, with $J=b_0P_O$ a constant mean open time is given as $\tau_O=1/b_0$.

For this model, there are two dissociation constants for the inhibitory Ca^{2+} binding, K_2 and K_4. At the bottom of Fig. 8(a), i.e., without any IP_3 bound, the dissociation constants for four inhibitory Ca^{2+} bindings all equal K_4, and at the top of Fig. 8(a), i.e., with four IP_3 bound, the dissociation constants for four inhibitory Ca^{2+} bindings all equal K_2. In between, with increasing number of IP_3 bindings, the dissociation constant K_4 at the most right side will be replaced by K_2 one by one.

The fittings of the channel model 8 to the experimental data are given in Figs. 8(b) and 8(c) for P_O, τ_O, and τ_C. It can be seen that this model can reproduce the following characteristics of the experimental data. (1) The model provides a flat P_O at optimal calcium concentration at I=10 μM. (2) The model gives a sensitive response of P_O to I at optimal C. (3) The model exhibits a steep increasing response and a steep decreasing response of P_O to C at saturating I. As shown in Table I, a small mismatch value is obtained for P_O fitting with this model. Thus, except for the 13-state model, this model gives the best fitting for the channel open probability among the seven models. However, compared to all other models discussed above, this model is much more complex.

VII. DISCUSSION

The IP$_3$R channel model plays a key role for the simulation of intracellular calcium signals. Different IP$_3$R models have been proposed in the past.[5–9,13–16,19,20] We here suggest that a proper IP$_3$R model should reflect the tetrameric structure of the channel and we fit the IP$_3$R patch clamp data

recorded in their native environment of the nuclear membrane. As an example, we consider the fitting of patch clamp data of IP_3R on the nuclear membrane in *Xenopus* oocytes. Different types of IP_3R models are discussed in the paper in order to fit the experimental data of the open probability, mean open time, and mean close time of the channel as a function of calcium concentration and IP_3 concentration. Our discussion indicates that rather than possessing four independent and identical subunits, an IP_3R channel shows a sequential binding-unbinding process with Ca^{2+} ions and IP_3 messengers. Our simulations also favor the assumption that a channel opens through a conformational transition from a close state to an active state.

At saturating IP_3 concentration stimulus, the observation that the channel shows a steep increase in open probability at small Ca^{2+} concentration favors a sequential binding of activating Ca^{2+} ions, while the observation that the channel shows a rapid decrease in open probability at large Ca^{2+} concentration favors a sequential binding of inhibitory Ca^{2+} ions. Similarly, the sensitivity of the channel open probability to small IP_3 stimuli requires a sequential binding dynamics of IP_3 messengers on the channel. At the optimal Ca^{2+} concentration, the open probability shows a flat behavior, which can be easily matched by assuming a conformational change with constant rates leading to the opening of the channel. Without the conformational change, a flat behavior can only be achieved at $P_O=1$ for the channel model.

By considering the tetrameric IP_3R which consists of four independent and identical subunits, both the number of model states and the number of model parameters can be largely reduced. This provides an advantage for any IP_3R simulations. However, if we consider a structurally symmetric channel with dynamically sequential binding IP_3R, both the number of model states and the number of model parameters are large. For example, if considering one IP_3 binding site and two Ca^{2+} binding sites for activating and inhibitory processes each, at least a 45-state channel should be implemented, which is similar to model 8. As a result, the sequential IP_3R model will complicate simulations.

On the other hand, relaxing requirements to obtain a handy model, one may consider that even a model as simple as model 2 can roughly fit the experimental data. Thus in some situations the model 2 may be sufficient for calcium signaling simulations. In that sense, in order to simplify the numerical process in the modeling, the De Young–Keizer model may still be regarded a good choice for calcium signaling studies.

For the De Young–Keizer model, model 1, we cannot fix the values of the binding rates a_3 and a_4 with stationary data of P_O, τ_O, and τ_C. A similar limitation that the steady state results of P_O, τ_O, and τ_C are not sufficient to determine all the binding parameters in the models holds also for the other seven models. In this paper, parameters of the models are chosen to fit the steady state experimental data, and the different models are compared based on such fittings. In Ref. 23, three IP_3R models have been compared by fitting them to the dynamic data of IP_3R responding to step increases in Ca^{2+} and IP_3 concentrations, rather than the stationary data at steady Ca^{2+} and IP_3 concentrations. With the original De Young–Keizer model, the peak of the bell-shaped curve moves to the right with increasing $[IP_3]$, while when the best-fit parameters are used in the De Young–Keizer model for dynamic data, a left moving peak is obtained. In biologically realistic situations, the IP_3R channels typically respond to oscillating Ca^{2+} concentration. It was argued in Ref. 23 that during an oscillation, the steady-state response is less important than the response to a changing Ca^{2+} concentration, and the receptors seldom experience a steady Ca^{2+} concentration except at resting state. Thus the important question is posed as to what extent the steady-state data should be used to constrain the parameter fitting of the model. On the other hand, another conclusion drawn in Ref. 23 is that time-dependent responses to steps of Ca^{2+} and IP_3 concentrations alone are insufficient to determine the model parameters unambiguously. Thus, a reasonable modeling approach in the future should incorporate both the steady state[11–13] and dynamic data.[24,25]

Here we did not address the kinetic feedback of calcium, i.e., the physiological condition that released calcium may bind back to the channel. As shown, for instance, in Ref. 26 such feedback leads to largely increased open probabilities and bursts of channel openings/closings. Under those conditions, details of the single channel model, such as the conformational transition, further affect gating dynamics. To give an example, release bursts for models with this transition may occur independent of momentary calcium concentration.[26] The bursts are therefore different from the bursts for earlier models, where the opening/closing transition involves calcium binding/unbinding. We expect that our kinetic parameter fittings will be useful for further analysis of integrative calcium release models.

ACKNOWLEDGMENTS

This work was supported by National Institutes of Health Grant No. 2R01GM065830-06A1 for J.S. and J.P. J.S. also acknowledges the support from the National Science Foundation of China under Grant No. 10775114.

[1]M. J. Berridge, P. Lipp, and M. D. Bootman, Nat. Rev. Mol. Cell Biol. **1**, 11 (2000).
[2]J. K. Foskett, C. White, K. H. Cheung, and D. O. Mak, Physiol. Rev. **87**, 593 (2007).
[3]J. Lechleiter, S. Girard, E. Peralta, and D. Clapham, Science **252**, 123 (1991).
[4]J. Sneyd and M. Falcke, Prog. Biophys. Mol. Biol. **89**, 207 (2005).
[5]G. W. De Young and J. Keizer, Proc. Natl. Acad. Sci. U.S.A. **89**, 9895 (1992).
[6]A. Atri, J. Amundson, D. Clapham, and J. Sneyd, Biophys. J. **65**, 1727 (1993).
[7]E. J. Kaftan, B. E. Ehrlich, and J. Watras, J. Gen. Physiol. **110**, 529 (1997).
[8]S. Swillens, P. Champeil, L. Combettes, and G. Dupont, Cell Calcium **23**, 291 (1998).
[9]J. Sneyd and J. F. Dufour, Proc. Natl. Acad. Sci. U.S.A. **99**, 2398 (2002).
[10]I. Bezprozvanny, J. Watras, and B. E. Ehrlich, Nature (London) **351**, 751 (1991).
[11]D. O. Mak and J. K. Foskett, J. Gen. Physiol. **109**, 571 (1997).
[12]D. O. Mak, S. McBride, and J. K. Foskett, Proc. Natl. Acad. Sci. U.S.A. **95**, 15821 (1998).
[13]D. O. Mak, S. M. McBride, and J. K. Foskett, J. Gen. Physiol. **122**, 583 (2003).
[14]I. Baran, Biophys. J. **84**, 1470 (2003).
[15]D. Fraiman and S. P. Dawson, Cell Calcium **35**, 403 (2004).

[16]J. Shuai, J. E. Pearson, J. K. Foskett, D. O. Mak, and I. Parker, Biophys. J. **93**, 1151 (2007).
[17]W. J. Bruno, J. Yang, and J. E. Pearson, Proc. Natl. Acad. Sci. U.S.A. **102**, 6326 (2005).
[18]J. Yang, W. J. Bruno, W. S. Hlavacek, and J. E. Pearson, Biophys. J. **91**, 1136 (2006).
[19]Y. Li and J. Rinzel, J. Theor. Biol. **166**, 461 (1994).
[20]J. Keizer and G. De Young, J. Theor. Biol. **166**, 431 (1994).
[21]B. Hille, *Ion Channels of Excitable Membranes*, 3rd ed. (Sinauer Associates, Sunderland, MA, 2001).
[22]I. Bezprozvanny, Cell Calcium **38**, 261 (2005).
[23]J. Sneyd, M. Falcke, J.-F. Dufour, and C. Fox, Prog. Biophys. Mol. Biol. **85**, 121 (2004).
[24]J.-F. Dufour, I. M. Arias, and T. J. Turner, J. Biol. Chem. **272**, 2675 (1997).
[25]D.-O. D. Mak, J. E. Pearson, K. P. C. Loong, S. Datta, M. Fernandez-Mongil, and J. K. Foskett, EMBO Rep. **8**, 1044 (2007).
[26]S. Rüdiger, J. W. Shuai, W. Huisinga, C. Nagaiah, G. Warnecke, I. Parker, and M. Falcke, Biophys. J. **93**, 1847 (2007).